RSC Advances

ROYAL SOCIETY OF CHEMISTRY

www.rsc.org/advances

Environmental benign enhanced hydrogen production via lethal H_2S under natural sunlight using hierarchical nanostructured Bismuth Sulfide

Orthorhombic bismuth sulfide nanomaterial of unique morphologies including nanorods, dandelion flower like hierarchical nanostructures were successfully synthesized by solvothermal method. Considering the tunable band gap of these nanostructures within visible region and near IR, photocatalytic hydrogen production under sunlight has been demonstrated. We observed excellent hydrogen production (8.899mmoleh^{-1}g^{-1}) under sunlight (on a sunny day between 11.30am to 2.30pm).

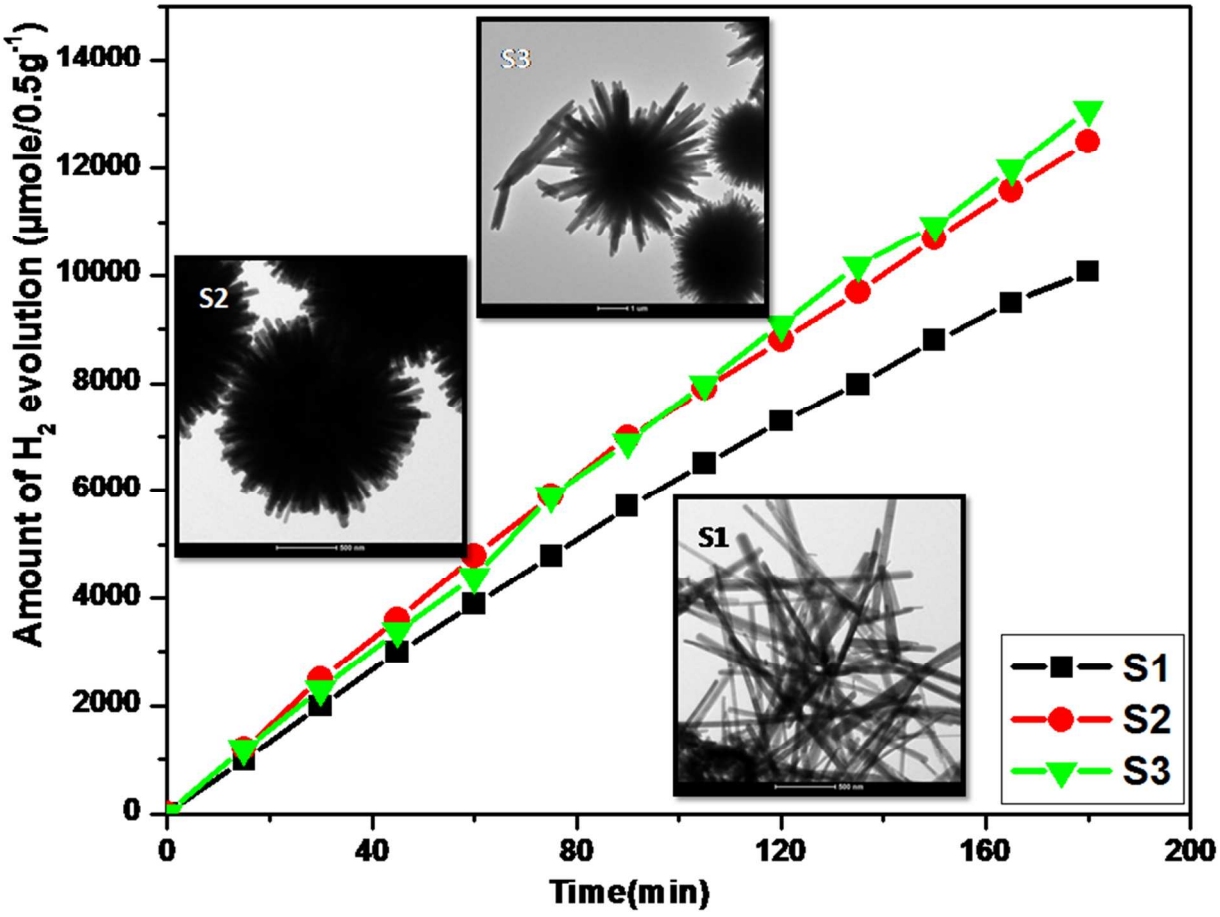

Journal Name

RSCPublishing

ARTICLE

Environmental benign enhanced hydrogen production via lethal H_2S under natural sunlight using hierarchical nanostructured Bismuth Sulfide

Cite this: DOI: 10.1039/x0xx00000x

U. V. Kawade, R. P. Panmand, Y. A. Sethi, M. V. Kulkarni, S. K. Apte, S. D. Naik, B. B. Kale*

Received 00th January 2012,
Accepted 00th January 2012

DOI: 10.1039/x0xx00000x

www.rsc.org/

The nanorods and hierarchical nanostructures (dandelion flower) of bismuth sulfide were synthesized by solvothermal method. The effect of solvent such as water and ethylene glycol on the morphologies and size of Bismuth sulfide were studied. The structural study shows the orthorhombic phase of bismuth sulfide. We have observed nanorods of size 30-50nm and dandelion flowers assembled with these nanorods. The formation mechanism of hierarchical nanostructures of bismuth sulfide has also been proposed. Considering the tuneable band gap of these nanostructures within visible region and near IR, photocatalytic hydrogen production from H_2S under normal sunlight has been demonstrated for the first. The abundantly available toxic H_2S has been utilised to produce hydrogen under normal sunlight. We observed an excellent hydrogen production i.e. 8.88 mmole g^{-1} h^{-1} under sunlight (on a sunny day between 11.30am to 2.30pm) for the Bi_2S_3 flowers and 7.08 mmole g-1 h-1 for nanorods. Hierarchical nanostructures supress the charge carrier recombination due to defects which ultimately responsible for higher activity. The hydrogen evolution obtained is quite stable when the catalyst has been used repeatedly. The hydrogen evolution via water splitting was observed to be lower than H_2S splitting. The bismuth sulphide was observed to be good eco-friendly visible light active photocatalyst under natural sunlight. Photoresponse study shows that Bi_2S_3 microstructures are a good candidate for applications in high-sensitivity photo detectors and photo electronic switches.

1. Introduction

Considering the paramount significance of hydrogen (H_2) as a clean energy source, efforts have been made worldwide to investigate new methods for cheaper hydrogen production. Fujishima and Honda investigated the solar assisted water splitting using TiO_2 which opens new doors of solar energy conversion.[1] This photocatalytic process has attracted much attention and appears to be promising strategy for clean, low cost and environmentally hydrogen production by utilizing solar energy.[2-4(a)] The photo cleavage of H_2S to H_2 and S has immense importance because of its waste disposal and environment problem. Acidic H_2S is a product of oil refineries, which is toxic and corrosive in nature and creates the environmental problems. The currently used Claus process has limitations and is utilizing only negligible amount of H_2S for preparation of liquid sulphur for agriculture and pharmaceutical industries. The photo-splitting of hydrogen sulphide for production of hydrogen and sulphur has significance as this reaction require less energy (79.9 kJ/mole) compared to photosplitting of H_2O (285.83 kJ/mole). Bismuth Sulfide is known to be effective for water splitting. There are very limited reports on the water splitting using Bi_2S_3 as a photocatalyst. [4(b)] Recently, we have demonstrated photocatalytic production of H_2 from H_2S using a variety of nanostructured photocatalyst.[5-10(e)] However, in commercial point of view, there is a need of search of a highly efficient stable catalyst. In this context, we have studied nanostructured Bi_2S_3 photocatalyst for H_2S splitting for hydrogen production.

Bi_2S_3 is a semiconductor material with direct band gap 1.3eV [11-13] has numerous potential applications in photovoltaic, IR spectroscopy and thermo-electric devices. It is also used for the synthesis of Zeolite, inorganic materials as an imaging agent in x-ray computed tomography and as a liquid junction solar cell. Particularly in photocatalysis, Bismuth sulfide has been used as photocatalyst for organic dye degradation in the composite form[14,15] The composites like Bi_2S_3/TiO_2, Bi_2O_3-Bi_2S_3 are also reported for photo electrochemical hydrogen evolution as well as photochemical hydrogen production from water.[16-19]

The photo electrochemical and photo response study was also reported.

Recently, due to encouraging properties of hierarchical nanostructures, research has been focused on the fabrication of controlled size, shape & hierarchically assembled nanostructures**.** Many researchers have studied different morphologies such as nanotubes, nanoparticles, [20] nanowires, [21,22] nanorods bundles and dandelion like nanostructure, [23] urchin like nanospheres [24] using various synthesis methods. However, the use of nanostructured bismuth sulfide as a visible light active photocatalyst has not been studied in detail for the hydrogen generation from H_2S splitting. More significantly, effect of nanostructures of Bi_2S_3 on the photocatalytic activity under sunlight has not been studied thoroughly. In view of this, we have demonstrated synthesis of bismuth sulfide nanostructures i.e. nanorods/hierarchical nanostructures and their photocatalytic activity.

In the present investigation, we report the photocleavage of waste H_2S to H_2 under normal sunlight by a Bi_2S_3 semiconductor photocatalyst which is hitherto unattempted. We also report the effect Bi_2S_3 nanostructures such as nanorods and hierarchical nanostructures on the production of hydrogen and its mechanism. The hydrogen evolution via water splitting has also been performed using these nanostructures. The structural and optical study of these nanostructures has been presented in detail.

2. Experimental

2.1. Material synthesis

All the reactants and solvents used in our experiments were analytical grade purchased from reputable firm. Bi_2S_3 nanostructures were prepared by dissolving 2 mmole of $Bi(NO)_3.5H_2O$ and 8 mmole of thiourea(TU) into 80ml solvent [in water and mixture of (1:3) water : ethylene glycol (EG)]. After stirring for one hour, the solution was transferred into a 100ml Teflon lined stainless steel autoclave. Then the system was sealed and kept in the oven at 150^0C. After reaction, the system was cooled to room temperature naturally and black precipitate obtained was filtered, washed with water and ethanol several times. The product was dried at 80^0C and further used for characterization. The sample **S1** was synthesized in water medium at 24 hrs. The samples **S2** and **S3** were synthesized in water: ethylene glycol (1:3) at 24hr and 30hrs, respectively.

2.2. Characterization

The structural investigation was performed using X-ray diffractometer (XRD, Model-D8, Advance, and Bruker AXS). The morphology was observed with FESEM (JEOL instrument, IIT Roorkee) and FESEM (Hitachi S-4800). The morphology and crystal size was also confirmed by Transmission electron microscopy (FEI-Technai). The optical study was performed using UV-visible spectrometer (PerkinElmer Model-lambda-950). Photoluminescence of the synthesized material was recorded on Horiba Fluorolog 3 spectrofluorometer. Single point BET surface area is measured using Quantachrome Instruments. The variation in current was measured by an electrometer workstation (Keithley Electrometer, 6517B) with illumination of light.

2.3. Photoresponse Properties

Experimental Setup for Measurements of Photo responsive Properties of Bi_2S_3 nanostructures in supporting information (See supporting information ESI I). A photo-response device was built with the as-synthesized Bi_2S_3 hierarchical microstructures following the device configuration shown in Fig. SI1. The ITO substrate of area 1 X 2 cm^2 is etched by dilute HF in 0.2 X 1 cm^2 in dimensions and then the ITO film is divided in two parts which act as duel electrodes (See figure SI 1). A white light LED lamp (of 8 mW/m^2) was used as the illumination source and a bias voltage (typically, 20 mV) was applied on the ITO electrode.

2.4. Photocatalytic study for H_2S splitting

The cylindrical quartz photochemical thermostatic reactor was filled with 700 ml 0.5 M water KOH and purged with argon for 1 h. Hydrogen sulfide (H_2S) was bubbled through the solution at the rate 2.5 ml min^{-1} at a 298 K. H_2S is continuously fed into the system during photo reduction. Bi_2S_3 was introduced into reactor and irradiated with normal solar light with constant stirring. The excess hydrogen sulfide was trapped in NaOH solution. The amount of hydrogen evolved was measured using a graduated gas burette. The experimental Setup for measurements of hydrogen production from H_2S under sunlight is shown in supporting information (See supporting information ESI II). Detail study explained in photocatalytic activity and measurement part.

2.5. Photocatalytic study for H_2O splitting

To evaluate the photocatalytic activity for hydrogen generation from water splitting, Xenon lamp ($\lambda \geq 430$ nm) is used as a visible light source. The photocatalyst was suspended into Quartz photochemical reactor with a water cooled quartz immersion well and a thermo stated water jacket. A high pressure Xenon lamp source of 300 Watt intensity with cutoff filter was used. At a constant temperature, the reactor containing catalyst with sacrificial agent Na_2S and Na_2SO_3, is vigorously stirred and purged with argon for 30mins. Each experiment is carried out using 0.5gm catalyst in 100 ml solution. The amount of hydrogen evolved analysed from gas chromatography (GC, Nucon, model 5765, India).

3. Results and Discussion

Fig 1 shows the XRD pattern of bismuth sulfide sample synthesized in (a) water medium- 24 hr (S1), (b) water: ethylene glycol (1:3)-24hr (S2) and (c) water: ethylene glycol (1:3)-30hr (S3), respectively. All the diffraction peaks are matching with the standard JCPDS data (No-060333). All the

planes were indexed which shows the pure orthorhombic phase of Bi_2S_3 and they are equally crystalline.

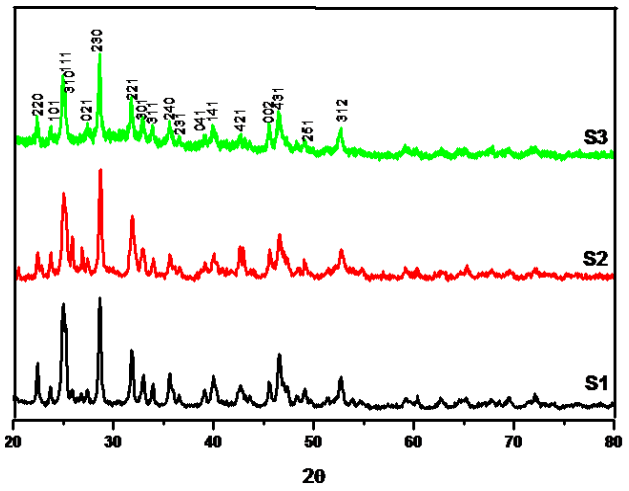

Fig 1- XRD of Bi_2S_3 synthesized by hydrothermal at 150^{0}C with different solvent: (a) water- 24 hr (S1), (b) water: ethylene glycol (1:3)24hr (S2) and (c) water: ethylene glycol (1:3) 30hr (S3).

The optical properties were investigated by UV-visible diffused reflectance spectroscopy. Fig 2 shows the UV-DRS spectrum of bismuth sulfide synthesized by solvothermal method using different solvents. The direct band gap of the Bi_2S_3 sample S1, S2 and S3 was observed to be 1.42, 1.48 and 1.45 eV respectively which is higher than bulk (1.3 eV).[11-13] The blue shift in band gap energy has been observed due to the nanocrystalline nature of the samples.

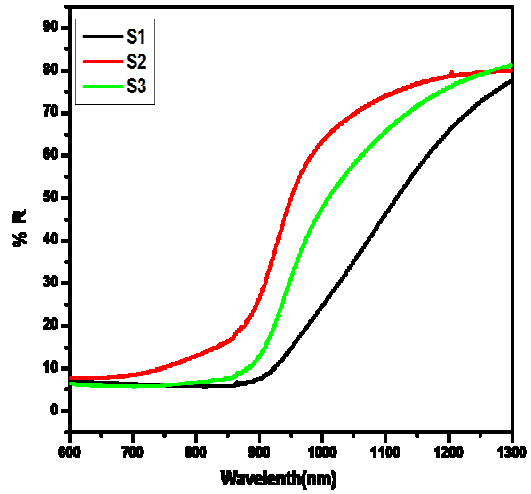

Fig. 2- UV-visible spectra of Bi_2S_3 synthesized by hydrothermal at 150^{0}C: (a) S1, (b) S2,(c)S3.

Fig 3 (a, b) shows the FE-SEM image of Bi_2S_3 prepared at 150^{0}C for 24hr (S1) in water medium. These images show the nanorods of 30-50 nm diameter and 2-4 µm in length. The nanorods are random in size and not aligned. In water medium, the growth of Bi_2S_3 is very fast and hence randomly distributed and uneven sized nanorods are observed.

When the reaction is carried out for 24 hrs in water: ethylene glycol (1:3) medium, hierarchical nanostructured dandelion flowers (c, d) of 1-2 µm in size were observed. The nanorods of size 20-50nm are self-aligned and orient to form flower like morphology. All nanorods grow radially out of the centre part. When the reaction was prolonged to 30 hrs, hierarchical nanostructured flowers (e, f) of size 2-4µm were formed by self alignment of nanorods of diameter 100-150nm. The flowers obtained are well defined, formed by self alignment of well separated nanorods (puffy) as compared to the Bi_2S_3 obtained within 24 hrs. It is quite obvious to have bigger flowers with higher diameter of nanorods because the crystal growth is favoured due to prolonged reaction time via Ostwald ripening phenomenon.[25]

TEM studies (Fig. 4) reveals the morphological variation in hierarchical Bi_2S_3 with solvent as discussed in earlier. Fig.4 (a) shows the Bi_2S_3 rods of size in the range of 30 to 50nm which also confirmed by the FESEM analysis. The corresponding ED pattern shows good crystallinity and d values calculated are matching with the XRD results. TEM of sample S2 (fig. 4(c)) and S3 (fig 4(e)) shows flower like morphology as discussed in FESEM. From TEM images, diameter of rods was observed to be consistent with FESEM investigations. The corresponding electron diffraction (ED) pattern also shows orthorhombic structure as per the calculated d values. The bright spots of ED pattern also show the single crystalline nature of the material.

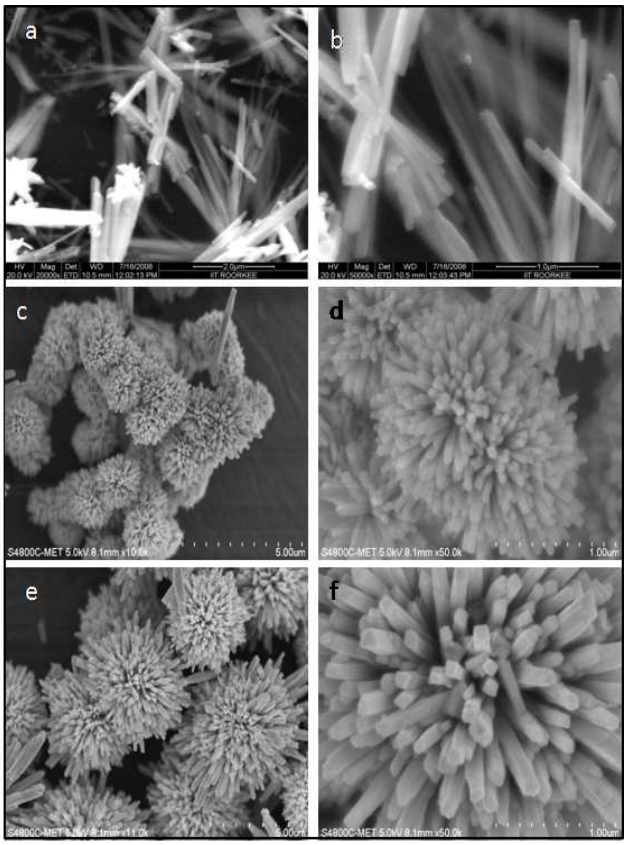

Fig 3 - FE-SEM images of the Bi_2S_3 synthesized by hydrothermal at 150^{0}C: (a, b) S1, (c, d) S2, (e, f) S3.

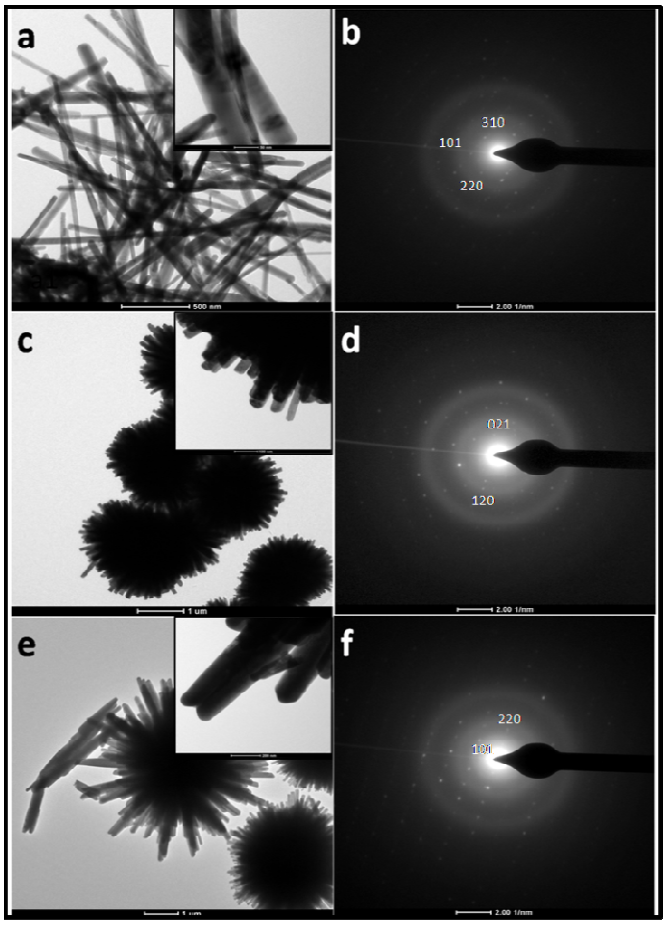

Fig 4 - TEM images of the Bi_2S_3 synthesized by hydrothermal at 150^0C: (a, b) S1, (c, d) S2, (e, f) S3.

Photoluminescence (PL) measurement of Bi_2S_3 was performed at room temperature with excitation wavelength of 450 nm (fig 5). The spectrum consists of one strong emission peak at 510nm that can be ascribed to high level transition in Bi_2S_3 semiconductor nanocrystallites. It is observed that all of the products have a peak around 510 nm. However, peak intensity in the case of urchin like flower morphology is less than nanorods. [27] This is due to the surface defects or surface states created by morphology and lower particle size. [28, 29]

4. Mechanism

The hydrothermal method provides uniform heating environment under pressure and simultaneous nucleation than the conventional methods due to its uniform heating effect. The solvents have an influence on the product morphologies and favour the synthesis of Bi_2S_3 with different pathways. The formation reaction may be described as follows.[26]

$Bi(NO_3)_3 + H_2O \leftrightarrow BiONO_3 + 2HNO_3$

$NH_2CSNH_2 + 2HNO_3 + 2H_2O \rightarrow H_2S + 2NH_4NO_3 + CO_2$

$2Bi(NO_3)_3 + 3H_2S \rightarrow Bi_2S_3 + 6HNO_3$

$2Bi(NO_3)_3 + 3NH_2CSNH_2 + H_2O \rightarrow Bi_2S_3 + 6NH_4NO_3 + 3CO_2$

The growth of Bi_2S_3 nanorods is accelerating via nucleation and crystal growth mechanism. Bi $(NO_3)_3$ hydrolyzes strongly in the water and reacting with TU. The strong complex action between Bi^{3+} and TU leads to the formation of Bi-TU complexes.[26,30] At the same time, HNO_3 react with thiourea and H_2S along with ammonium nitrate and carbon dioxide were formed. Prior to the hydrothermal process, the formation of H_2S is significantly slow but at high temperature and pressure formation of H_2S is increased. [31]

The Bi_2S_3 nuclei are formed by reaction of Bi^{3+} ions present in the solution and H_2S at hydrothermal condition. The further growth of Bi_2S_3 nuclei takes place due to prolong reaction time. Bi_2S_3 is a lamellar structure with links Bi_2S_3 units forming infinite chains parallel to the c-axis. The stronger covalent bond between the planes perpendicular to the c-axis facilitates higher growth rate along the c-axis. The much weaker Vander walls bonding between the planes perpendicular to the a-axis limits the growth of the nanorods in horizontal direction and facilitate their cleavage to form one dimensional nanostructure.[31]

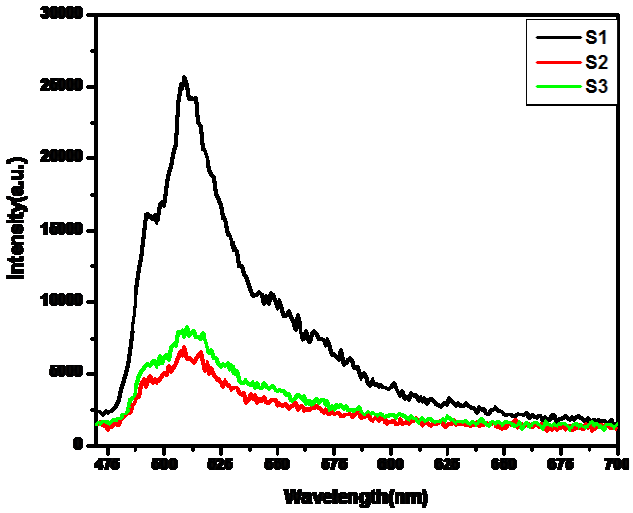

Fig 5 - PL spectra of the Bi_2S_3 sample S1, S2 and S3

Whereas, in our reaction, when Ethylene Glycol (EG): water used as reaction medium then EG acts as a co-ordination agent. Bismuth nitrate and Thiourea was dissolved in mixed solvent (EG and water) under magnetic stirring respectively. When two solutions were mixed together no precipitation was observed and solution was yellowish and transparent under stirring unlike water system. This might be attributed to the co-ordination of EG.[32,33] The employ of EG, complex of bismuth produced with hydroxide via the coordination. In the solvothermal process because of temperature and pressure, the complex gradually decomposed to release the bismuth ions. The Bi_2S_3 nuclei are formed by reaction of Bi^{3+} ions present in the solution and H_2S at solvothermal condition.

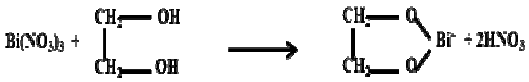

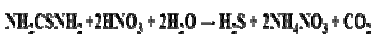

It is indicated that both TU and EG plays an important role in the formation of hierarchical nanostructures i.e. flower. The TU complexes are favourable for the oriented growth of the nanorods and also acted as a ligand in the formation of flower.[26] As well as powder synthesized in water and mixed solvent (water: ethylene glycol) were benefit of forming nanorods and hierarchical flowers, respectively. The high viscosity substance is able to modify the mobility of the particles in suspension as well as collision rates. Ethylene glycol in the solution implies high adsorption on the inorganic substances, which is able to induce the steric hindrance.[34] probably this chemical event leads to a minimizing in the growth process, causing reduction in particle size. The interface energy with high surface tension between Bi_2S_3 and mixed solvent (water: ethylene glycol) is higher as compared to water. This interface energy and high surface tension[35,36] are also promoting the formation of well, self aligned and organized flower like morphology. Hence, the nanorods formation by water mediated reaction and hierarchical nanostructures i.e. flowers by water: ethylene glycol (1:3) mediated reaction is quite understood.

5. Photoresponce

The Photoresponse of the obtained Bi_2S_3 nanorods (S1) as well as Bi_2S_3 micro flowers (S2 and S3) was measured as a function of time using the white light source (Figure 6). The current increased by 1.06X for S1 (nanorods) and 1.44X and 1.65X for S2 and S3 (micro flowers) upon exposure to white light (Figure a, b and c). After switching off the lamp, the current was instantaneously fallen down to original value. The on/off cycles could be repeated many times without any detectable degradation in current, indicating that all three Bi_2S_3 samples could be reversibly switched between low and high conductivity. The I-V curves measured at a large bias range for the micro flowers under light and dark conditions are shown in Figure 6 (e –f), which shows that the slope of the I-V curve became higher when the light was on, indicating an enhanced conductivity. However, microflower (sample S3) shows increase in slope compared with sample S2. In case of the nanorods, there was also a slight increase in the slope of the I-V curve after switching on the light; however, the increase in the slope of the I-V curve was not significant as compared to the both microflowers samples (Figure 6d). In these cases, the energy from the light, excited the electrons in the semiconductor Bi_2S_3 from the valence band into the conduction band, increasing the charge carrier concentration via direct electron-hole pair creation and thus enhancing the conductivity of the materials.[37] It is obvious that the conductivity of the Bi_2S_3 microflowers is more sensitive to the white light exposure than the nanorods. It is believed that the multiple internal reflections of light within the interior voids of the microflowers are responsible for the enhanced photoresponsive sensitivity of the microflower structure than nanorods.[38] Particularly, for microflowers (sample S3) has slight enhancement in photoresponse than sample S2 and it may be due to change in nature of flower. These results suggest that the prepared hierarchical Bi_2S_3 microstructurs are a good candidate for applications in high-sensitivity photo detectors and photo electronic switches.

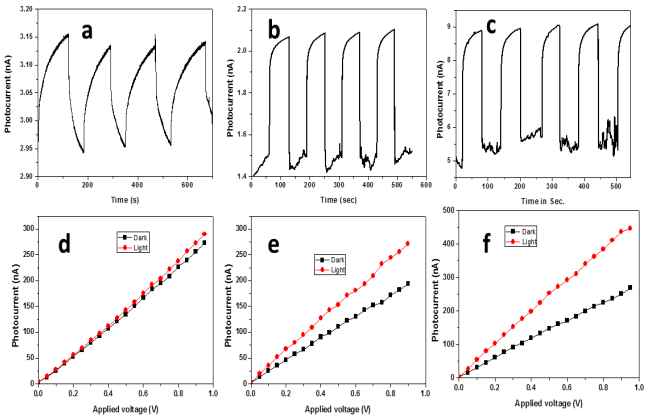

Fig 6- The Photoresponse with time at a bias of 50 mV (a, b, c) and I-V curves (d, e, f) of Bi_2S_3nanorods (S1) (d) and microflowers (S2 (e) and S3 (f))

6. Photocatalytic activity and measurement

Bismuth sulfide is a semiconductor with band gap 1.3-1.7ev and because of its good spectral response to solar light; the photocatalytic activities of bismuth sulfide have been investigated. Here, we have reported extremely high hydrogen evolution from H_2S splitting under solar light irradiation especially for hierarchical nanostructured bismuth sulfide flowers as compared to rods (Table 1). The photocatalytic activities of the as synthesized Bi_2S_3 were evaluated without further treatment under direct sunlight. In 0.5M KOH solution, the weaker, diprotic acid H_2S dissociates and maintains equilibrium with hydrogen disulfide HS^- ions. The sulfide semiconductor absorbs light and generates electron hole pairs. The photo generated valance band hole (h^+_{VB}) after band gap excitation of powder of Bi_2S_3 oxidizes the HS^- ion to disulfide ion (S_2^{2-}), liberating a proton from HS^- ion. The conduction band electron (e^-_{CB}) from Bi_2S_3 photocatalyst reduces protons to produce molecular hydrogen.[10]

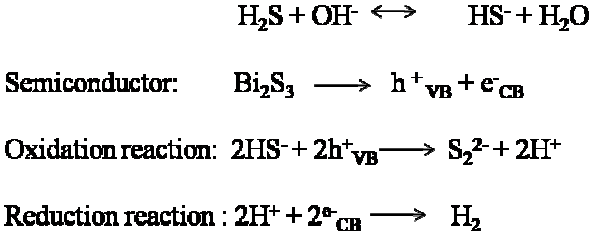

The photocatalytic hydrogen evolution reaction was performed using as synthesized nanostructures Bi_2S_3 under ambient condition. Different series of experiments were performed to compare the hydrogen evolution rate by bismuth sulfide synthesized by different solvent and the results along with BET surface are summarized in Table 1. The maximum hydrogen evolution i.e. 8.88 mmole g^{-1} h^{-1} was obtained using hierarchical nanostructured bismuth sulphide (sample S3) is higher (20%) than that of bismuth sulfide (S1) nanorods [7.08 mmole g^{-1} h^{-1}]. However, the sample S2 shows slightly less (2%) hydrogen evolution compared to sample S3. Both are hierarchical flower like structure and had good hydrogen evolution but due to puffy nature, sample S3 gives slightly higher evolution rate. PL study clearly shows the lower intensity broad peaks due to surface defects and states created by the hierarchical structure which ultimately supress the charge carriers recombination resulting into higher photocatalytic activity. Also, the hydrogen evaluation rate via H_2S splitting using sample S3 is better than other reported one. The comparative study of H_2 generation using Bi_2S_3 nanostructures and other reported metal sulphide nanocatalyst also performed and is shown in Table. (See supporting information ESI III). Though the $ZnIn_2S_4$ has good photocatalyst but is very expensive and the hydrogen evolution reported using xenon lamp and in the present study, we used natural sunlight. All other catalysts are cadmium based (toxic) and also showed hydrogen evolution under xenon lamp. However, still they show lower activity as compared to present Bismuth sulphide nanostructures. If we see the FESEM and TEM images of sample S1 carefully, the rods of different size with agglomeration have been observed which ultimately reduces the effective surface sites available for photoreaction. This is responsible for getting slightly lower hydrogen evolution in case of sample S1.

Figure 8 shows a typical time course of hydrogen evolution from water splitting using sample S1, S2 and S3 under visible light. Hydrogen evolution was not observed without light irradiation (kept for 2 hrs**)** Further, upon irradiation of light, only hydrogen was evolved steadily with time. The maximum hydrogen evolution i.e.0.019mmole$g^{-1}h^{-1}$, was obtained using hierarchical nanostructured bismuth sulphide(S3) which is higher than sample S1 and S2 [0.012 and 0.017 mmole g^{-1} h^{-1}]. Since, the reaction was carried out in the presence of sacrificial agent Na_2S and Na_2SO_3, an electron donor and the Oxygen was not evolved. The GC analysis showed absence of O_2 as well as N_2 from air.

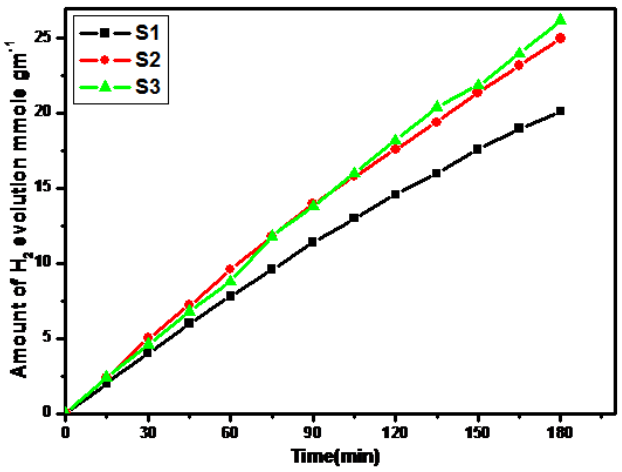

Fig 7 - Hydrogen evolution using sample S1, S2 and S3 Bi_2S_3 via H_2S Splitting

Fig. 7 and fig 8 shows the time dependent hydrogen evolution using as synthesized nanostructured bismuth sulfide. The linearity in the graph clearly shows the stable evolution rate of nanostructured Bi_2S_3. We performed the GC of evolved hydrogen gas during reaction and is given in supporting information (See supporting information ESI IV).

The hierarchical nanostructure flowers are self-oriented where effective surface sites have been increased due to their puffiness and also suppress the charge carriers recombination at the surface. In a solid, the charge carries repeatedly scatters off defects. Therefore, they do not accelerate faster instead of it

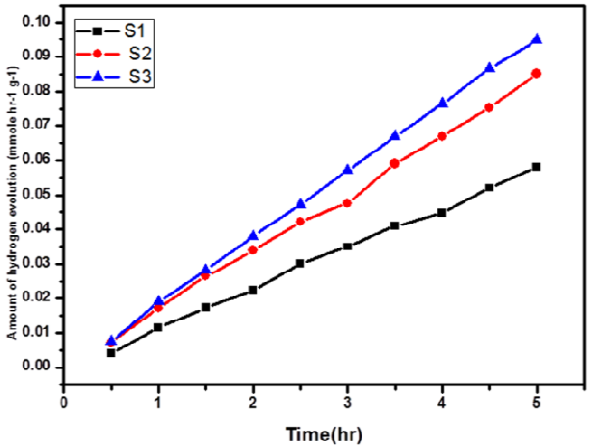

Fig 8 - Hydrogen evolution using sample S1, S2 and S3 Bi_2S_3 via H_2O Splitting

moves with a finite average velocity, called the drift velocity. This net carrier motion is usually much slower than the normally occurring random motion and hence rate recombination is slower which effective to achieve enhance photocatalytic activity of material. The electron transport to the surface might be increasing due to puffiness and hence sample S3 gives more hydrogen evolution. Whereas, sample S2 shows slightly little hydrogen evolution rate this may be due to compact hierarchical flower like morphology.[10] From the PL

study, it is observed that flower like morphology has more surface defects which enhance the charge carrier separation which also confirmed by Photoresponse study discussed in previous section. This could also be one of the reasons for obtaining high photocatalytic activity for Bi_2S_3 flowers.

Table 1: BET surface area and Relation of rate of hydrogen evolution to different solvent of synthesized Bi_2S_3.

Sample	S1	S2	S3
BET surface area (m^2/g)	3.71	9.82	6.63
H_2 via H_2S splitting $mmoleg^{-1}\ h^{-1}$	7.08	8.64	8.88
H_2 via H_2O splitting $mmoleg^{-1}\ h^{-1}$	0.012	0.017	0.019

The stability of the photocatalyst S1, S2 and S3 has also been examined by reusing the photocatalyst samples (after H_2S splitting). XRD of reused catalyst (RS1, RS2 and RS3) did not show a change in the phase purity of bismuth sulfide (See supporting information ESI V). The hydrogen evolution of reused catalyst (RS1, RS2 and RS3) is also shown in supporting information (ES VI). The hydrogen evolution rate by H_2O splitting is quite low as compared to that of H_2S splitting. It is noteworthy that the bismuth sulfide is a good photocatalyst for the production of hydrogen from H_2S.

Conclusions

In summary, we have demonstrated the fabrication of single crystalline nanorods and hierarchical nanostructures by simple "one pot" solvothermal method. The water mediated reaction gives nanorods and mixed solvent (water: ethylene glycol) mediated reaction confer hierarchical nanostructures (flower) of bismuth sulfide. The high interface energy and surface tension created are responsible for such flower like morphology. The as prepared Bi_2S_3 photocatalyst exhibited higher photocatalytic activity for H_2 evolution by H_2S splitting under normal sunlight. Excellent photocatalytic activity for hydrogen production via H_2S splitting under normal sunlight has been obtained. It is noteworthy that hierarchical nanostructured Bi_2S_3 i.e. dandelion flowers show significant H_2 evolution rate without any promoters. The hydrogen evolution from water splitting was also observed for all samples where flower like Bi_2S_3 shows higher hydrogen as compared to other structures.

Acknowledgements

The authors would like to thank to Department of electronics and information technology (DeitY), New Delhi for financial support. Also, thank Executive Director, C-MET, Pune and Nanocrystalline Material group, C-MET, for supporting this work.

Centre for Materials for Electronics Technology (C-MET), Panchwati, Pune-411 008.
Department of Electronics and Information Technology (DeitY), Government of India, New Delhi, INDIA.
Email: bbkale@cmet.gov.in/ kbbb1@yahoo.com

Electronic Supplementary Information (ESI) available.

References

1 A. Fujishima,K. Honda, *Nature*, 1972, **238**, 37.
2 J. Sun, G. Chen, G. Xiong, H. Pei Dong, *International Journal of Hydrogen Energy* 2013, **38**, 10731.
3 Q. Xiang, J. Yu, M. Jaroniec, *Journal of American Chemical society* 2012,**134**, 6575.
4 (a) K. M. Parida, S. Pany, Naik, B. *International Journal of Hydrogen Energy*, 2013, **38**, 3545**;** (b) C. Li, W. Chen, J. Yuan, M. Chen, W. Shangguan, *World Journal of Nano Science and Engineering*, 2011, **1**, 79.
5 S.Apte, S.Garaje, G. Mane, A. Vinu, S.Naik, D. Ambalnerkar, B. Kale, *Small*, 2011,**7**,957.
6 A. Bhirud**,** N. Chaudhari**,** L. Nikam**,** R. Sonawane**,** K. Patil**,** J Baeg**,** B. Kale**,** *International Journal of Hydrogen Energy***,** 2011**,** ***36*****,** 11628.
7 A. Bhirud, D. Shivaram, Sathaye. R. Waichal, L.Nikam, B. Kale, *Green Chemistry*, 2012,**14,** 2790.
8 S. Garaje, S. Apte, S. Naik, J. Ambekar, R. Sonawane, M. Kulkarni, A. Vinu, B. Kale, *Environmental Science and Technology*, 2013,**47,**6664.
9 S. Apte, S. Garaje, M. Valant, B. Kale, *Green Chemistry,* 2012,**14**, 1455.
10 **(a)** N. Chaudhari, A. Bhirud, R.Sonawane, L. Nikam, S. Warule, V. Rane, B. Kale, *Green Chemistry*, 2011, 13, 2500. (b)B. B. Kale, J. O. Baeg, K. Kong, S. Moon, L. K. Nikam and K. R. Patil *Journal of Materials Chemistry* 2011, **21**, 2624; (c) S. K. Apte, S. N. Garaje, S. S. Arbuj, B. B. Kale, J. O. Baeg, U. P. Mulik, S. D. Naik, D. P. Amalnerkar and S. W. Gosavi *Journal of Materials Chemistry*, 2011, **21**, 19241; (d) S. N. Garaje , S. K. Apte , S. D. Naik, J. D. Ambekar , R. S. Sonawane, M. V. Kulkarni , A. Vinu and B. B. Kale *Environmental Science and Technology*, 2013, 47 , 6664; (e) B. B. Kale, J. O. Baeg, S. M. Lee, H. Chang, S.-J. Moon and C. W. Lee *Advanced Functional Materials* 2006, **16**, 1349.
11 Song, C.; Wang, D.; Yang, T.; Hu, Z. *Crystal Engineering comm*. 2011, **13**, 3087.
12 G. Konstantatos L. Levina, J. Tang, E. Sargent, Nanoletters, 2008, **8**, 4002.
13 L. Li, N. Sun, Y. Huang, Y. Qin, N. Zhao, J. Gao, M. Li, H. Zhou, L. Qi,. *Advanced Functional Materials*, 2008,**18**,1194.
14 Z. Liu, W. Huang, Y. Zhang, Y. Tong, *Crystal Engineering Comm*, 2012**, 14**, 8261.
15 C. Li, W. Chen, J. Yuan, M. Chen, W. Shangguan, *World Journal of Nano Science and Engineering*, 2011, **1**, 79.
16 R.Brahimi, Y. Bessekhouad, A. Bouguelia, M. Trari, *Catalysis Today*, 2007,**122**, 62.
17 F. Liu, Y. Yang, J.Liu, W.Huang, Z. Li, *Journal of Electro analytical Chemistry*, 2012, **665**, 58.
18 J. Kim, M. Kang, *International journal of hydrogen energy,* 2012, *37*, 8249.
19 Y. Bessekhouad, M. Mohammedi, M. Trari, *Solar Energy Materials and Solar Cells*, 2002,**73,** 339.
20 A. Tahir, M. Ehsan, M. Mazhar, K. Upul, W. Zeller, A.D Hunter, *Chem. Mater*, 2010, **22**, 5084.
21 L. Cademartiri, F. Scotognella, P. O'Brien, B. Lotsch, J. Thomson, S. Petrov, N. Kherani, G. Ozin, *Nanoletters,* 2009, **9**,1482.
22 Y. Yu, W. Sun, *Materials Letters*, 2009, **63,** 1917.
23 L. Dong, Y. Chu, W. Zhang, *Materials Letters*, 2008, **62**, 4269.

24 X. Zhou, H. Shi, B. Zhang, X. Fu, K. Jiao, *Materials Letters*, 2008, **62**, 3201.
25 M. Ibanez, P. Guardia, A. Shavel, D. Cadavid, J. Arbiol, J. Morante, A. Cabot, *Journal of Physical Chemistry C*, 2011, **115**, 7947.
26 C. Tang, C. Wang, F. Su, C. Zang, Y. Yang, Z. Zong, Y. Zhang, *Solid State Sciences,* 2010, **12,** 1352.
27 Y. Xu, Z. Ren, G. Cao, W. Ren, K. Deng, Y. Zhong, *Physical B*, 2010, ***405***, 1353.
28 X. Zhu, J. Ma, Y. Wang, J. Tao, B. Lin, Y. Ren, X. Jiang, J. Liu, *Ceramics International*, 2008,***34*** , 249.
29 C. Tang, J. Su, Q. Hu, Y. Yang, C. Wang, C. Zhao, C Zang, Y. Zhang, *Solid State Sciences,* 2011, **13**,1152.
30 T. Thongtem, A. Phuruangrat, S.Wannapop, S. Thongtem, *Material letters*, 2010, **64**, 122.
31 M. Niasari, D. Ghanbaria, F. Davara, *Journal of Alloys and Compounds*, 2009, **488**, 442.
32 G. Tian, Y. Chen, W. Zhou, K. Pan, Y. Dong, C. Tian, H. Fu, *Journal of material chemistry,* 2011, **21**, 887.
33 M. Shang, W. Wang, H. Xu *Crystal Growth and Design, **2009,** **9**,* 991.
34 V.S.Marques, L.S. Cavalacante J.C. Sczancoski F.P. Alcantara, M.O. Orlandi, E. Moraes, J.A.LongoVarela, M.S.Li M.R.M.C.Santos, *Crystal Growth and Design,* 2010**,10,**4752
35 G.Zhu, P. Liu, J. Zhou, X. Bian, X. Wang, J. Li, Chen, B.; *Materials Letters*, 2008, ***62***, 2335
36 V.S. Marques, L.S. Cavalcante, J.C. Sczancoski, A.F.P. Alcantara, M.O.Orlandi, E.Moraes, E. Longo, A. VarelaJ. M. SiuLi, M.R.M.C. Santos, *Crystal Growth and Design,* 2010**, 10**, 4752.
37 H. F. Bao, X. Q. Cui, C.M. Li, Y. Gan, J. Zhang, J. Guo. *Journal of physical chemistry C,* 2007, **111**, 12279.
38 L. Lianshan, R. Cao, Z. Wang, J. Li, L. Qi. *Journal of physical chemistry C,* 2009, **113**, 18075.

